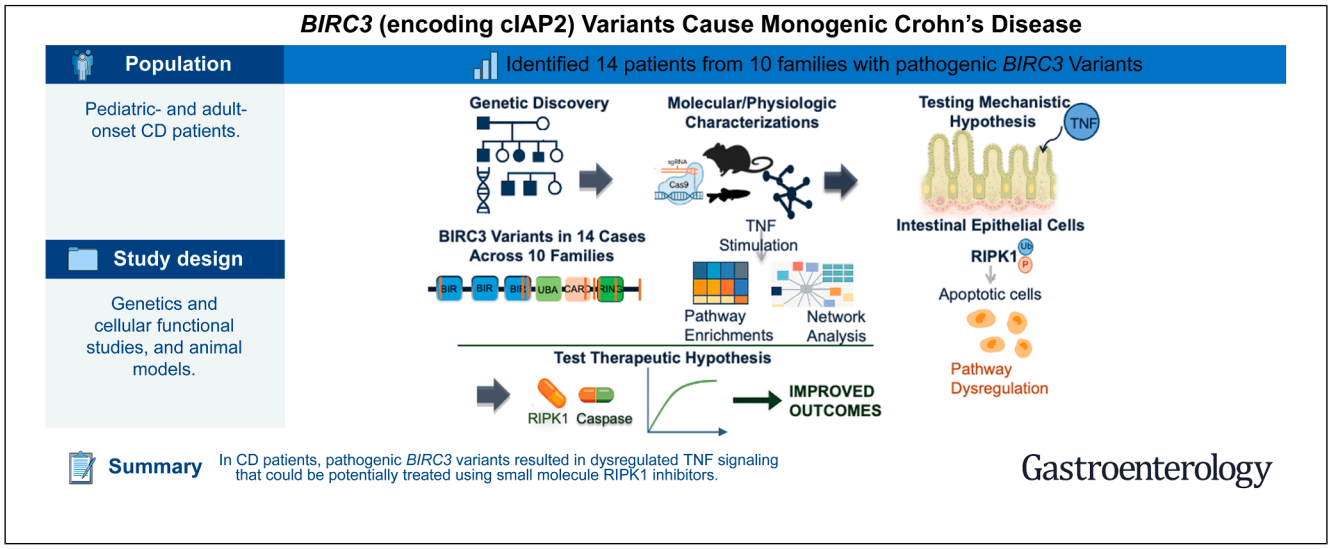
Gastroenterology 2026;171:885–901

INFLAMMATORY BOWEL DISEASE

BIRC3 (Encoding cIAP2) Variants Result in Dysregulated RIPK1 Signaling Leading to Increased Epithelial Cell Death and Are Associated With Monogenic Crohn's Disease

Qi Li,[1,*] **Ryusuke Nambu**,[1,2,*] **Hu Yaqiang**,[3,*] **Xiang Shen**,[4,*] **Carmen Argmann**,[5,*] **Rei Guan**,[1,*] **Erin Janssen**,[6,*] **Tom Le Voyer**,[7,8,9,*] Neil Warner,[1] Daniel D. Yu,[1] Jing Guo,[1,10] Kelvin Long,[1] Jodie Ouahed,[11] Michael Field,[11] Lauren Collen,[11] Jonas Bibus,[4] David Illig,[4] Meino Rohlfs,[4] Ziqi Yu,[4] Shaohong Yang,[12] Wenjuan Li,[1] Craig D. Platt,[13] Phillip H. Comella,[5] Daniel Jordan,[5] Mayte Suárez-Fariñas,[5] Mohammed F. Alosaimi,[14] Lauren A. Peters,[5] Jeremie Rosain,[8,9,15] Claire Fieschi,[7] Anne Puel,[8,9] Elena W. Y. Hsieh,[16,17] Takeo Naito,[18] Zhiyang Zeng,[19] Marta Velasco Rodríguez-Belvís,[20] Laura Palomino,[20] Peter Küster,[21] Dalin Li,[12] Christoph Klein,[4,22] Scott B. Snapper,[11,23] Jean-Laurent Casanova,[8,9,24,25] Raif Geha,[13] Edward Hoffenberg,[26] **Dermot P. B. McGovern**,[12,§] **Eric Schadt**,[5,§] **Daniel Kotlarz**,[4,22,27,§] **Dali Li**,[3,§] and **Aleixo M. Muise**[1,28,§]

[1]Cell and Systems Biology Program, Research Institute, Hospital for Sick Children, Toronto, Ontario, Canada; [2]Center for Pediatric Inflammatory Bowel Disease, Division of Gastroenterology and Hepatology, Saitama Children's Medical Center, Saitama, Japan; [3]Shanghai Frontiers Science Center of Genome Editing and Cell Therapy, Shanghai Key Laboratory of Regulatory Biology, East China Normal University, Shanghai, China; [4]Dr. von Hauner Children's Hospital, Department of Pediatrics, University Hospital, Ludwig Maximilian University Munich, Munich, Germany; [5]Department of Genetics & Genomic Sciences, Icahn School of Medicine at Mount Sinai, New York, New York; [6]Division of Pediatric Rheumatology, Michigan Medicine, Ann Arbor, Michigan; [7]Immunopathology Department, Saint-Louis Hospital, AP-HP, Paris, France; [8]Laboratory of Human Genetics of Infectious Diseases, Necker Branch, Institut National de la Santé et de la Recherche Médicale, and Imagine Institute, Paris Cité University, Paris, France; [9]St. Giles Laboratory of Human Genetics of Infectious Diseases, Rockefeller Branch, The Rockefeller University, New York, New York; [10]Department of Pediatrics, Shengjing Hospital of China Medical University, Shenyang, Liaoning, China; [11]Division of Gastroenterology, Hepatology, & Nutrition, Department of Pediatrics, Boston Children's Hospital, Harvard Medical School, Boston, Massachusetts; [12]F. Widjaja Foundation Inflammatory Bowel Research Institute, Cedars-Sinai Medical Center, Los Angeles, California; [13]Division of Immunology, Department of Pediatrics, Boston Children's Hospital, Harvard Medical School, Boston, Massachusetts; [14]Immunology Research Laboratory, College of Medicine, King Saud University, Riyadh, Saudi Arabia; [15]Study Center for Immunodeficiencies, Necker Hospital for Sick Children, Paris, France; [16]Division of Allergy and Immunology, Departments of Pediatrics and Internal Medicine, Children's Medical Center Dallas, University of Texas Southwestern, Dallas, Texas; [17]Department of Immunology, University of Texas Southwestern, Dallas, Texas; [18]Division of Gastroenterology, Tohoku University Graduate School of Medicine, Sendai, Japan; [19]Fengxian Central Hospital Affiliated to Southern Medical University, Shanghai, China; [20]Sección de Gastroenterología y Nutrición Pediátrica, Hospital Infantil Universitario Niño Jesús, Madrid, Spain; [21]Department of Paediatrics, Clemens Hospital GmbH Münster, Munster, Nordrhein-Westfalen, Germany; [22]German Center for Child and Adolescent Health (DZKJ), Partner Site Munich, Munich, Germany; [23]Division of Gastroenterology, Hepatology, and Endoscopy, Brigham & Women's Hospital, Harvard Medical School, Boston, Massachusetts; [24]Department of Pediatrics, Necker Hospital for Sick Children, Assistance Publique-Hôpitaux de Paris, Paris, France; [25]Howard Hughes Medical Institute, New York, New York; [26]Department of Pediatrics, Children's Hospital Colorado, University of Colorado Anschutz Medical Campus, Aurora, Colorado; [27]Institute of Translational Genomics, Helmholtz Munich, German Research Center for Environmental Health, Neuherberg, Germany; and [28]Departments of Pediatrics, Institute of Medical Science, and Biochemistry, University of Toronto, Toronto, Ontario, Canada



BACKGROUND & AIMS: Tumor necrosis factor (TNF) is a key driver of intestinal epithelial inflammation. The baculoviral inhibitor of apoptosis protein repeat-containing 3 (*BIRC3*) gene encodes the cellular inhibitor of apoptosis protein 2 (cIAP2), a known regulator of TNF signaling. Although genetic variants in components of the TNF signaling pathway have been reported, no human *BIRC3* variants have been previously identified. **METHODS:** We screened exomes obtained from Crohn's disease (CD) patients from multiple centers for *BIRC3* variants. We used cellular, mouse organoids, induced pluripotent stem cells–derived intestinal organoids, knock-in and knockout mouse models, and knockout zebrafish, as well as transcriptome analysis of various samples to determine pathogenicity of *BIRC3* variants. **RESULTS:** Rare and damaging *BIRC3* variants were identified in 14 patients from 10 unrelated families with CD diagnosed between infancy and adulthood. Functional studies showed that *BIRC3* deficiency caused impaired receptor-interacting protein kinase 1 (RIPK1) ubiquitylation, leading to RIPK1 autophosphorylation resulting in increased epithelial cell death. The p.H312Y cIAP2 variant identified in both our index and in another independent patient was mislocalizaed, and a knock-in mouse model of this *BIRC3* variant (cIAP2$^{H312Y/+}$) had exacerbation of chemically induced colitis, whereas ciap1$^{-/+}$ zebrafish developed spontaneous colitis. Transcriptome analysis of mice organoids and zebrafish showed that *BIRC3* deficiency led to inappropriate sustained activation of TNF-responsiveness genes in the absence of stimuli. Small molecule pharmacologic inhibition of RIPK1 or caspases attenuated intestinal inflammation in *BIRC3*-deficient intestinal organoids and cIAP2$^{H312Y/+}$ mice. **CONCLUSIONS:** We establish *BIRC3* deficiency as a cause of monogenic CD in both pediatric- and adult-onset patients and identify RIPK1 as a therapeutic target.

Keywords: Monogenic IBD; RIPK1; cIAP2; *BIRC3*.

Crohn's disease (CD), a form of inflammatory bowel disease (IBD), is characterized by a chronic relapsing and remitting disease course with transmural inflammation affecting any part of the gastrointestinal tract. The worldwide prevalence of CD continues to increase across all age-groups, including children and adolescents, placing a significant burden on health care systems in industrialized, newly industrialized, and emerging regions.[1] In IBD, tumor necrosis factor-α (TNF-α) is a key driver of intestinal epithelial inflammation. In rare cases, CD can result from pathogenic variants[2–4] in genes encoding regulators of TNF signaling, including *RIPK1*,[5–7] *CASP8*,[8] *IKBKG* (*NEMO*),[9] and *BIRC4*.[10]

Inhibitors of apoptosis (IAPs) are a highly conserved family of baculoviral inhibitor of apoptosis (IAP) repeat-containing genes that in mammalians include *BIRC2* and *BIRC3*, encoding the cellular IAPs (cIAP1 and cIAP2, respectively), and *BIRC4* (encoding X-linked IAP, XIAP). These IAPs are critical signaling molecules that regulate programmed cell death. Although cIAP1 and cIAP2 both have putative roles in mediating TNF signaling (reviewed by Lalaoui and Vaux[11] and Darding and Meier[12]), cIAP2 is also inducible and regulates innate immune inflammatory responses, and cIAP2 knockout mice exhibit resistance to

*** Authors share co-first authorship; § Authors share co-senior authorship.**

Abbreviations used in this paper: **AD, autosomal dominant; AR, autosomal recessive; BIRC3, baculoviral inhibitor of apoptosis protein repeat-containing 3; Cas9, clustered regularly interspaced short palindromic repeats-associated protein 9; CD, Crohn's disease; cIAP2, cellular inhibitor of apoptosis protein 2; CRISPR, clustered regularly interspaced short palindromic repeats; DEG, differential expression gene; DSS, dextran sulfate sodium; GSVA, gene set variation analysis; HEK, human embryonic kidney; IAPs, inhibitors of apoptosis; IBD, inflammatory bowel disease; iPSC, induced pluripotent stem cells; mRNA, messenger RNA; Nec-1, necrostatin 1; RIPK1, receptor-interacting protein kinase 1; RNA-seq, RNA sequencing; SMAC, second mitochondria-derived activator of caspases; TNF, tumor necrosis factor; WT, wild-type.**

Most current article

© 2026 The Author(s). Published by Elsevier Inc. on behalf of American Gastroenterological Association Institute. This is an open access article under the CC BY-NC-ND license (http://creativecommons.org/licenses/by-nc-nd/4.0/).
0016-5085
https://doi.org/10.1053/j.gastro.2026.05.022

lipopolysaccharide-induced sepsis due to macrophage apoptosis.[13] Previous studies have demonstrated that mice expressing enzymatically inactive cIAP1/2 died during embryonic development due to dysregulated receptor-interacting protein kinase 1 (RIPK1)–mediated apoptosis,[14] and cIAP2-deficient mice exhibit increased susceptibility to chemically induced colitis.[15,16]

Although biologics, such as anti-TNF antibodies, and small molecules are now standard treatment for CD,[17] these therapies are typically selected empirically rather than being tailored to a patient's specific molecular defect. However, the identification of monogenic causes of intestinal disease has resulted in novel targeted therapeutic options for patients.[18–21] Here, we describe pediatric- and adult-onset CD patients with pathogenic *BIRC3* variants leading to dysregulated TNF signaling and identity RIPK1 inhibition as a small molecule targeted therapy.

WHAT YOU NEED TO KNOW

BACKGROUND AND CONTEXT

In rare cases, Crohn's disease can result from pathogenic variants in genes encoding regulators of tumor necrosis factor, a key driver of intestinal inflammation.

NEW FINDINGS

We describe 14 patients from 10 independent families with pediatric- and adult-onset Crohn's disease carrying pathogenic *BIRC3* (encoding cellular inhibitor of apoptosis protein 2) variants. This novel form of monogenic inflammatory bowel disease leads to dysregulated receptor-interacting protein kinase 1–dependent tumor necrosis factor signaling in intestinal epithelial cells.

LIMITATIONS

These studies primarily focused on the role of cellular inhibitor of apoptosis protein 2 in regulation of receptor-interacting protein kinase 1 and intestinal epithelial cell homeostasis; however, cellular inhibitor of apoptosis protein 2 deficiency may also contribute to disease pathogenesis through functions in non-epithelial cells.

CLINICAL RESEARCH RELEVANCE

This study highlights the therapeutic potential of targeting dysregulated cell death pathways through receptor-interacting protein kinase 1 inhibition not only patients in with *BIRC3* deficiency but also those with tumor necrosis factor-related forms of monogenic Crohn's disease, and potentially in a subset of polygenic Crohn's disease characterized by similar transcriptional profiles.

BASIC RESEARCH RELEVANCE

Functional studies using human induced pluripotent stem cell–derived intestinal organoids, animal models, and cell lines showed that cellular inhibitor of apoptosis protein 2 deficiency resulted in dysregulated receptor-interacting protein kinase 1-dependent signaling in the intestinal epithelial and cell death. Overall, reduced cellular inhibitor of apoptosis protein 2 expression was effectively mimicking chronic tumor necrosis factor stimulation leading to the development of Crohn's disease.

Materials and Methods

Study Participants

Written informed consent was obtained from participants and/or their guardians in accordance with local regulations in Germany, France, and the United States, with approval from the appropriate Institutional Review Boards.

Animal Studies

All animal studies followed the Animal Research: Reporting of In Vivo Experiments (ARRIVE) guidelines.

Generation of cIAP2$^{H312Y/+}$ and cIAP2$^{-/-}$ Mouse Models

We generated the knock-in cIAP2$^{H312Y/+}$ mice (equivalent to the H312 variant in human cIAP2) and knockout cIAP2$^{-/-}$ mice (as a result of a 1 nucleotide deletion at amino acid position 313, resulting in a frameshift and premature stop codon at amino acid position 375) by microinjection of clustered regularly interspaced short palindromic repeats (CRISPR)-associated protein 9 (Cas9) messenger (m)RNA, single-guide RNA, and single-stranded oligodeoxynucleotides (GenScript) into zygotes, as described previously.[22,23]

Briefly, super ovulated C57BL/6J female mice were mated with male mice, and 1-cell embryos were collected from oviducts. Cas9 mRNA (50 ng/μL), single-guide RNA targeting the cIAP2 loci (50 ng/μL), and single-stranded oligodeoxynucleotides (10 ng/μL) carrying the desired point variants were coinjected into the pronuclei of the embryos. The injected embryos were cultured in potassium simplex optimized medium before they were transplanted into pseudopregnant mice. Two weeks after birth, genomic DNA from the tail of the newborn founder (F0) mice was extracted for sequencing. Mice were housed in standard cages in a specific pathogen-free facility on a 12-h light/dark cycle with ad libitum access to food and water.

Generation of ciap1$^{-/+}$ Zebrafish Model

To generate ciap1$^{-/+}$ mutant zebrafish, as previously described,[4] guide RNA (AACATGCCAAGTGGTTTCCA) was designed on CHOPCHOP[24] and synthesized using the HiScribe T7 High Yield RNA Synthesis Kit (E2040L, New England Biolabs), following the manufacturer's instructions. Cas9 mRNA was in vitro synthesized from pT3TS-nCas9n plasmid (a gift from Wenbiao Chen, Addgene, Cat no. 46757) using the mMESSAGE mMACHINE T3 Transcription Kit (Invitrogen, Cat no. AM1348), following the manufacturer's instructions. Next, each AB embryo was injected with 100 pg of guide RNA, 150 pg of Cas9 mRNA, and 20% phenol red. Once the F0 fish reached adulthood, they were outcrossed to AB to screen for potential founders.

Differentiation of Induced Pluripotent Stem Cells Into Colon Organoids

Human induced pluripotent stem cells (iPSC) were generated by the iPSC core facility at the German Research Center for Environmental Health (Supplementary Methods).

RNA Sequencing Differential Gene Expression Analysis of Mouse Intestinal Organoids

Transcriptomic data were generated on 2 independent experiments (either triplicate or duplicate measures per condition) for a total of 30 samples, with 29 remaining after quality control. Genomic alignment of paired-end RNA sequencing (RNA-seq) reads to the Genome Reference Consortium Mouse Build 38 reference genome was performed using HISAT2 software with default parameters. Gene-level quantification was conducted using featureCounts, also with default settings. Multimapping reads were flagged and discarded. Genes with low expression were filtered using edgeR's filterByExpr() function based on the experimental design before normalization and linear modeling.

After filtering, count data were normalized via the weighted trimmed mean of M values.[25] Normalized counts were transformed via the voom-transformation and were the final input for statistical modeling. Statistical analysis was done using the Limma framework[26,27] in R 4.3.3 (R Foundation for Statistical Computing) software and its available packages, as described previously[28] and in the Supplementary Methods.

RNA Sequencing Differential Gene Expression Analysis in Zebrafish

Human orthologs of zebrafish differentially expressed genes were determined using the Drosophila RNAi Screening Center (DRSC) integrative ortholog prediction tool (DIOPT 8.5/9.0).[29] Multimapped genes were removed and only high-ranking orthologs kept. At adjusted $P < .05$, 116 down-regulated and 305 up-regulated differential expression genes (DEGs) were identified, and after converting to human orthologs, we identified 71 down-regulated and 210 up-regulated genes.

Gene Set Enrichment Analysis

Enrichment analyses were done using the Fisher's exact test, unless otherwise stated, with P values adjusted using a Benjamini-Hochberg multiple test correction (significant if adjusted $P < .05$) procedure. Gene Set Enrichment Analysis[30] was also performed using Gene Set Enrichment Analysis 4.3.2 software, and the preranked function (t statistic) with 1000 permutations. Canonical pathways included hallmark (version 2023.2.Hs.symbols); and Reactome (version 2022). Gene sets related to IBD genome-wide association study,[31] monogenic IBD genes,[32] and anti-TNF response vs nonresponse[33,34] were curated from cited resources. As indicated, either normalized enrichment scores or significance was presented in heat map (negative log-adjusted P value) using the R package pheatmap or dot plot using R package ggplot2.[35]

Network Analysis

Bayesian Gene Regulatory Networks can capture fundamental properties of complex systems in states that give rise to complex (diseased) phenotypes.[36] Bayesian Gene Regulatory Networks were generated as previously reported[28] from colonic biopsy specimen RNA-seq data (Mount Sinai Crohn's and Colitis Registry CD subset using intestinal expression quantitative trait loci information as priors).[37] The network included both inflamed and uninflamed biopsy specimens and was constructed using Reconstructing Integrative Molecular Bayesian Network (RIMBANet) software[38] and visualized using Cytoscape 3.7.[39] To evaluate the BIRC3-centered subnetwork in the context of anti-TNF therapy, we quantified activity of the subnetwork (gene set variation analysis [GSVA] R package) in gut transcriptomic data from the A Safety and Efficacy Study for Infliximab (Remicade) in Patients With Ulcerative Colitis (ACT1) infliximab clinical trial in adult ulcerative colitis (GSE23597)[34] and compared levels between infliximab responders and nonresponders (see Supplementary methods).

Functional Assay

Several functional assays were used and are outlined in the Supplementary Material.

Results

Identification of BIRC3 Variants in Crohn's Disease Patients

Exome sequencing of our index patient (patient 4), a young boy who presented with typical CD features (oral ulcers, perianal disease, and granulomatous ileo-colonic inflammation) identified a heterozygous de novo *BIRC3* variant (NM_001165: c.934C>T) that resulted in a novel cIAP2 p.H312Y protein not reported in any database (Figure 1*A* and Table 1). Subsequent screening of CD patients for rare *BIRC3* variants revealed 13 additional individuals from 9 unrelated families (diagnosed between <1 and 31 years of age), including patient 5, who presented at 12 years of age and carried the same heterozygous p.H312Y cIAP2 variant as the index proband. Although pediatric- or adult-onset CD patients carried heterozygous cIAP2 variants (p.T35A, p.P266R, p.H312Y, p.C557X, and p.D530H), 3 sibling pairs from independent consanguineous families harbored homozygous cIAP2 variants (p.Y522X, p.C588Y, and p.X605Rext10) and presented in infancy (Figure 1*B*).

All *BIRC3* variants were localized to highly conserved regions (Figure 1*C*), rare (novel or gnomAD[40] allele frequency <0.00001), damaging (Combined Annotation Dependent Depletion [CADD] Score[41] >15), and were classified as either likely pathogenic or as variants of unknown significance based on the American College of Medical Genetics and Genomics/Association for Molecular Pathology classification[42] (Table 1).

Crohn's Disease-Associated cIAP2 Variants Result in Dysregulated RIPK1-Dependent Cell Death in Intestinal Epithelial Cells

To determine the functional significance of the identified cIAP2 variants in TNF signaling, we overexpressed all of the cIAP2 variants in human embryonic kidney (HEK293T) cells. Upon TNF stimulation, all cIAP2 variants exhibited increased apoptosis as measured by elevated caspase-3/7 levels using a Caspase-Glo 3/7 assay (Promega Corporation) (Figure 2*A*). Furthermore, overexpression of the cIAP2 variants in HEK293T cells resulted in reduced

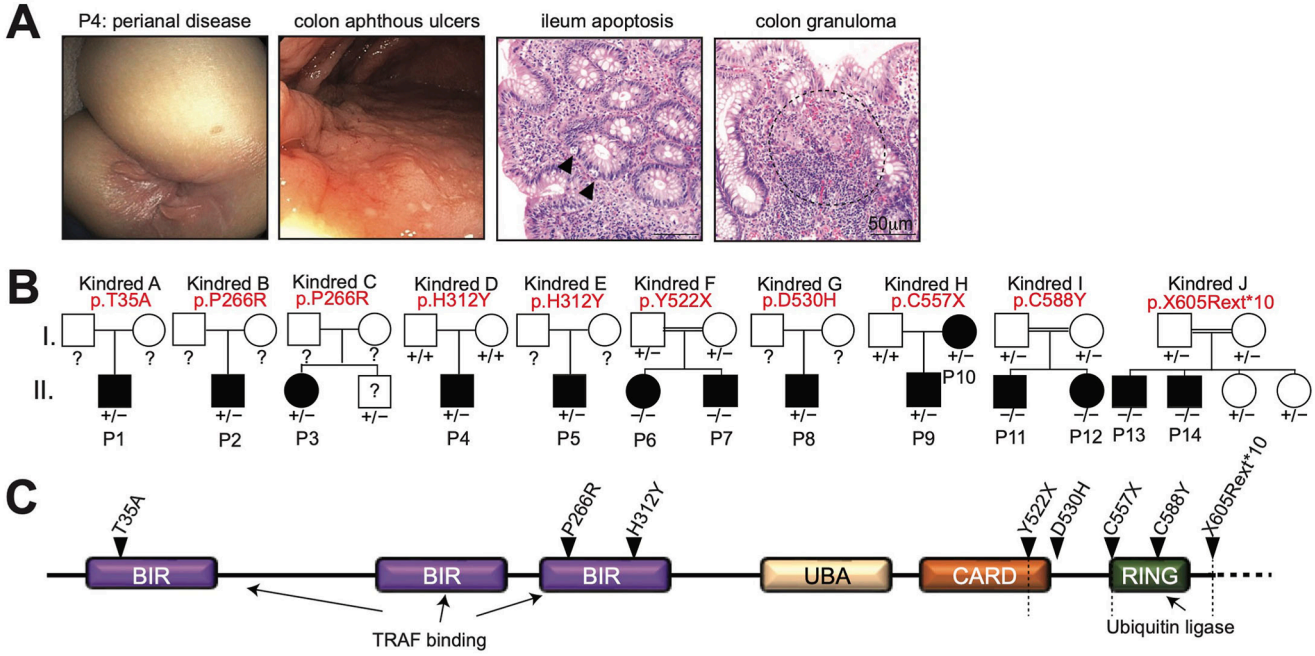


Figure 1. Clinical features and genetics studies of BIRC3 deficiency. (*A*) Clinical phenotype of index patient (P) 4 showing perianal disease (*left*), aphthous ulcers (*middle*), and H&E-stained ileal sections showing apoptosis (*black arrows*, *middle*), and ileal granuloma (*dashed circle*) with plasmacytosis (*right*). (*B*) Pedigrees of the kindreds. Circles represent female and squares represent male members. Filled shapes represent the CD phenotype. "+" WT, "−" variant, "?" genotype and phenotype unknown. (*C*) Structure of the cIAP2 protein indicating the position of patient variants. CARD, caspase recruitment domain; TRAF, TNF receptor–associated factor; UBA, ubiquitin-associated.

RIPK1 ubiquitylation when stimulated with TNF (Figure 2*B*) and serine 166 (S166) RIPK1 autophosphorylation when costimulated with TNF and the second mitochondria-derived activator of caspases (SMAC) mimetic BV6 (Figure 2*C*) compared with wild-type (WT) cIAP2.

To further model the patient-specific effects in a physiologically relevant model, we generated CRISPR-engineered human iPSC-derived intestinal organoids with cIAP2 knockout (cIAP2$^{-/-}$) or knock-in of several patient variants (H312Y, Y522X, and X605Rext10) (Figure 2*D*), as well as the cIAP2 knockout HCT116 cells and reconstituted them with overexpression of the above-mentioned variants. Similar S166 RIPK1 autophosphorylation was observed in these human iPSC-derived intestinal organoids (Figure 2*D*) and HCT116 cells (Supplementary Figure S1*A*) expressing either cIAP2 knockout (cIAP2$^{-/-}$) or knock-in of the patient-associated cIAP2 variants upon costimulation with TNF/BV6.

In support of cIAP2's role in regulating RIPK1-dependent signaling, after TNF treatment, quantitative polymerase chain reaction analysis showed elevated expression of proinflammatory *CCL5* and *CCL20* chemokines in HCT116 cells with knockout of cIAP2 or lentiviral knock-in of several patient-associated cIAP2 variants compared with WT (Supplementary Figure S1*B*). Furthermore, we demonstrate that overexpression of all patient-associated cIAP2 variants increased *CCL20* in HEK293T cells upon TNF stimulation (Supplementary Figure S1*C*). Cotransfection of WT cIAP2 in HEK293T cells overexpressing all the patient-derived variants demonstrated a dose-dependent partial rescue of apoptosis as measured by caspase-3/7 activity after TNF treatment, indicating loss of function rather than a dominant-negative effect (Figure 2*E*). Furthermore, in HeLa cells, the H312Y, T35A, and X605Rext*10 cIAP2 variants under TNF/BV6 stimulation exhibited distinct punctate, indicating a trafficking defect may be responsible for the loss of function for these cIAP2 variants (Figure 2*F*).

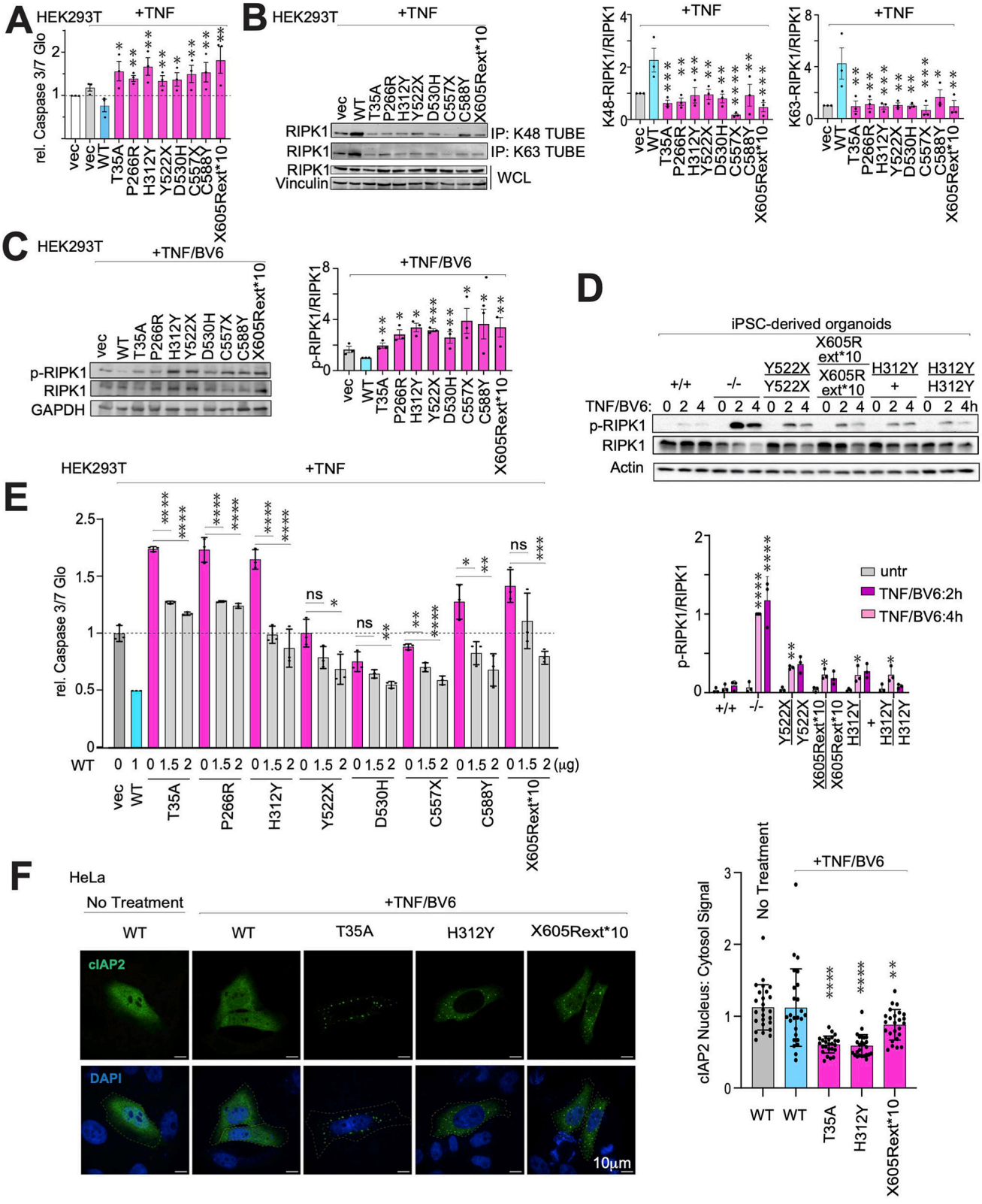
cIAP2$^{H312Y/+}$ Mice and ciap1$^{+/-}$ Zebrafish Exhibit Inflammation With Enhanced Intestinal Epithelial Apoptosis

To further investigate the effects of the patient-associated *BIRC3* variants on intestinal inflammation, we generated CRISPR-engineered zebrafish and mouse knockout models as well as a knock-in mouse model harboring the (cIAP2$^{H312Y/+}$) equivalent to the human heterozygous cIAP2 p.H312Y protein variant identified in 2 independent families with CD (see Materials and Methods and Supplementary Figure S2*A*–*D*). cIAP2$^{H312Y/+}$ mice showed no overt intestinal abnormalities and were phenotypically indistinguishable from WT cIAP2$^{+/+}$ littermates (Supplementary Figure S2*E*). However, when challenged with 3% dextran sulfate sodium (DSS), the cIAP2$^{H312Y/+}$ mice developed exacerbated colitis as evidenced by increased Disease Activity Index and shortened colon length compared with cIAP2$^{+/+}$ WT littermates (Figure 3*A*).

Table 1. *BIRC3* Genetic Variant Characteristics and Patient Crohn's Disease Phenotype and Treatment

Patient number	P1	P2	P3	P4	P5	P6	P7	P8	P9	P10	P11	P12	P13	P14
Kindred	A	B	C	D	E		F	G	H		I		J	
Amino acid position	p.T35A		p.P266R	p.H312Y			p.Y522X	p.D530H	p.C557X		p.C588Y		p.X605Rext*10	
Nucleotide position	c.103A>G		c.797C>G	c.934C>T			c.1566T>A	c.1588G>C	c.1671T>A		c.1763G>A		c.1813T>C	
Allele status	Hetero		Hetero	Hetero			Homo	Hetero	Hetero		Homo		Homo	
Variant annotation														
Chromosome	11		11	11			11	11	11		11		11	
Position (GRCh38)	102324612		102325306	102325546			102336207	102336768	102336958		102337050		102337100	
dbSNP151	…		rs201026275	…			…	rs749715948	rs774719063		…		…	
Position (GRCh37)	102195343		102196037	102196277			102206938	102207499	102207689		102207781		102207831	
gnomADv4 maf	Novel		0.00002975	Novel			Novel	6.22E-07	6.23E-07		Novel		Novel	
COSMIC	…		…	1			…	…	…		…		…	
CADD_phred (GRCh37-v1.6)	25.3		25.0	27.1			34.0	22.2	36.0		27.0		16.1	
Clinical presentation														
IBD classification	CD	CD	CD	CD	CD	CD	CD	CD	CD	CD	CD	CD	CD	CD
Age of IBD onset, *y*	20	17	3	4	12	9	0.6	12	0.8	31	1	0.8	0.1	0.5
Sex	Male	Male	Male	Male	Male	Female	Male	Male	Male	Female	Female	Female	Male	Male
Consanguinity	N/A	N/A	No	N/A	N/A		Yes	N/A	No		Yes		Yes	
Disease location	N/A	Ileo-colonic	Ileo-colonic	Ileo-colonic	Ileo-colonic	Ileo-colonic, esophagus	Ileo-colonic	Ileo-colonic	Ileo-colonic	Colonic	Ileo-colonic	Colonic	Colonic	Colonic
Stricturing	N/A	Yes	Yes	No	N/A	No	No	No	No	No	No	No	No	No
Perianal disease	N/A	Yes	Yes	Yes	Yes	No	No	Yes	No	No	No	No	No	No
Fever	N/A	No	No	Yes	N/A	No	Yes	N/A	N/A	N/A	Yes	Yes	No	No
Skin inflammation	N/A	No	No	No	N/A	No	Yes	N/A	Yes	N/A	No	No	No	No
Joint inflammation	N/A	No	No	No	N/A	No	No	N/A	Yes	N/A	No	No	No	Yes
Recurrent infections	N/A	No	No	No	N/A	No	No	N/A	N/A	N/A	Yes	Yes	No	No
Surgery and therapy (chronological order first used)	N/A	N/A	Colectomy, abdominoperineal resection Mesalamine, AZA, IFX, ADA	IFX + MTX	N/A	Mesalamine	Colectomy IFX	N/A	N/A	N/A	VDZ + AZA	VDZ + AZA	UST	UST
ACMG classification	LP		VUS	LP			LP	LP	LP		LP		LP	

ACMG, American College of Medical Genetics and Genomics; AZA, azathioprine; CADD, Combined Annotation Dependent Depletion; COSMIC, Catalogue Of Somatic Mutations In Cancer; IFX, infliximab; LP, likely pathogenic; MTX, methotrexate; N/A, not available; UST, ustekinumab; VDZ, vedolizumab; VUS, variant of unknown significance.


A
HEK293T
+TNF
rel. Caspase 3/7 Glo
vec
vec
WT
T35A
P266R
H312Y
Y522X
D530H
C557X
C588Y
X605Rext*10
B
HEK293T
+TNF
RIPK1
RIPK1
RIPK1
Vinculin
IP: K48 TUBE
IP: K63 TUBE
WCL
K48-RIPK1/RIPK1
K63-RIPK1/RIPK1
C
HEK293T
+TNF/BV6
p-RIPK1
RIPK1
GAPDH
p-RIPK1/RIPK1
D
iPSC-derived organoids
+/+
-/-
Y522X Y522X
X605R ext*10 X605R ext*10
H312Y +
H312Y H312Y
TNF/BV6: 0 2 4 0 2 4 0 2 4 0 2 4 0 2 4 0 2 4h
p-RIPK1
RIPK1
Actin
E
HEK293T
+TNF
rel. Caspase 3/7 Glo
WT 0 1 0 1.5 2 0 1.5 2 0 1.5 2 0 1.5 2 0 1.5 2 0 1.5 2 0 1.5 2 0 1.5 2 (μg)
p-RIPK1/RIPK1
untr
TNF/BV6:2h
TNF/BV6:4h
F
HeLa
No Treatment
+TNF/BV6
WT
WT
T35A
H312Y
X605Rext*10
cIAP2
DAPI
10μm
cIAP2 Nucleus: Cytosol Signal
No Treatment
+TNF/BV6

Histopathologic examination using H&E-stained colon sections showed severe intestinal inflammation in cIAP2$^{H312Y/+}$ mice, including distortion of tissue architecture, infiltration of inflammatory cells, edema in the lamina propria area, as well as apoptotic cells throughout the colon and small intestine (Figure 3*B*). Consistent with increased epithelial cell death, cleaved caspase-3 (CASP3) staining was markedly elevated throughout the intestine of DSS-treated cIAP2$^{H312Y/+}$ mice (Figure 3*C* and *D*). Of note, our index patient 4 with the p.H312Y cIAP2 variant also exhibited increased apoptosis in intestinal biopsy specimens (Figure 1*A*).

In contrast to mice and humans, zebrafish possess a single cellular *birc* gene (*birc2* encoding ciap1),[43] an ortholog of both human *BIRC2* and *BIRC3* genes. Knockout of *birc2* in zebrafish (ciap1$^{-/-}$) resulted in lethality within 4 days after birth, whereas heterozygous ciap1$^{-/+}$ zebrafish survived but developed spontaneous intestinal inflammation in adulthood. Histologic analysis (H&E and alcian blue staining) of the ciap1$^{-/+}$ zebrafish showed epithelial damage, infiltration of inflammatory cells, and loss of architecture compared with ciap1$^{+/+}$ zebrafish (Figure 3*E* and *F*). Additionally, immunofluorescence revealed increased casp8 staining in the intestinal epithelium of adult ciap1$^{-/+}$ zebrafish, indicating increased cell death (Figure 3*G*).

Integrative Molecular Analysis Identifies BIRC3 as a Driver of TNF-Associated Transcriptional Activation and Altered TNF Responsiveness

To define the transcriptional consequences of cIAP2 perturbation, RNA-seq was performed on mouse intestinal organoids derived from cIAP2$^{+/+}$ (WT), cIAP2$^{H312Y/+}$, and cIAP2$^{-/-}$ mice under basal conditions and after TNF stimulation. In unstimulated conditions, cIAP2$^{-/-}$ organoids exhibited widespread DEG relative to WT (Figure 4*A*; Supplementary Tables ST1-2). The cIAP2$^{H312Y/+}$ organoids displayed a similar but attenuated transcriptional profile, with significant DEGs strongly enriched within the cIAP2$^{-/-}$ DEG set (fold enrichment, 3.9; $P = 6.8 \times 10^{-05}$) (Supplementary Table ST3).

Direct comparison of basal cIAP2$^{-/-}$ and cIAP2$^{H312Y/+}$ log2 fold changes demonstrated moderate concordance in transcriptional directionality (Pearson's $r = 0.36$, $P < 2 \times 10^{-16}$) (Figure 4*B*), indicating a shared biological program. Linear regression across all genes yielded a slope of 0.28, indicating that heterozygous organoids retain ∼28% of the transcriptional amplitude observed in knockout organoids, suggesting a gene dosage–dependent hypomorphic phenotype. We observed that untreated organoids from cIAP2$^{H312Y/+}$ and cIAP2$^{-/-}$ mice effectively mimicked the DEGs from TNF-stimulated cIAP2$^{+/+}$ organoids with ∼35% of TNF-stimulated genes in WT organoids already induced in untreated cIAP2$^{-/-}$ organoids (fold enrichment, 3.35; $P = 1.5 \times 10^{-94}$) (Supplementary Table ST3). Gene Set Enrichment Analysis using the TNF-stimulated cIAP2$^{+/+}$ organoids up-regulated gene set confirmed significant enrichment in both cIAP2$^{-/-}$ and cIAP2$^{H312Y/+}$, organoids (Figure 4*C* and Supplementary Table ST4), indicating constitutive activation of TNF-responsive pathways in the absence of stimulation.

Upon TNF stimulation, both cIAP2$^{-/-}$ and cIAP2$^{H312Y/+}$ organoids induced TNF-responsive gene signatures, as reflected by strong positive normalized enrichment scores (Figure 4*C* and Supplementary Table ST4). However, interaction modeling comparing TNF responses in cIAP2 models relative to cIAP2$^{+/+}$ organoids demonstrated a general blunted TNF effect (Figure 4*C* and *D* and Supplementary Table ST1). Interaction volcano plots revealed impaired amplification of TNF signaling in the context of reduced cIAP2 activity. These findings suggest that although cIAP2 deficiency creates a chronically primed inflammatory state, it simultaneously reduces the dynamic range of acute TNF responsiveness.

Consistent with this pattern, hallmark pathway analysis showed that inflammatory, interferon-γ, interleukin 6–Janus kinase–signal transducer and activator of transcription protein 3, and apoptosis-related programs were induced in cIAP2$^{-/-}$ organoids under basal and upon TNF treatment but showed reduced enrichment in the differential TNF treatment comparisons (Figure 4*E*, Supplementary Table ST5). These pathways were also enriched in DEGs identified from RNA sequence analysis of ciap$^{-/-}$ zebrafish compared with WT ciap$^{+/+}$ controls, validating the mouse

Figure 2. Functional studies of *BIRC3* deficiency. (*A*) Caspase-3/7 activity assay of overexpressed cIAP2 constructs in HEK293T cells, with or without TNF stimulation (n = 3 biological replicates). *Error bars*: mean ± standard error (SE). Unpaired *t* test, **P* < .05, ***P* < .01. (*B*) K48 and K63 tandem ubiquitin binding entities (TUBE) assays and quantification of RIPK1 ubiquitination in HEK293T cells overexpressing cIAP2 variants after 2 hours of TNF stimulation (n = 3 biological replicates). *Error bars*: mean ± SE. One-way analysis of variance (ANOVA), **P* < .05, ***P* < .01, ****P* < .001, *****P* < .0001. (*C*) Western blot assays and quantification of RIPK1 Ser166 phosphorylation (p-) in HEK293T cells overexpressing cIAP2 variants after 6 hours of TNF/BV6 stimulation (n = 3 biological replicates). GAPDH, glyceraldehyde-3-phosphate dehydrogenase. *Error bars*: mean ± SE. Unpaired *t* test, **P* < .05, ***P* < .01, ****P* < .001. (*D*) Western blot assays and quantification of serine 166 p-RIPK1 in human iPSC-derived organoids after TNF/BV6 treatment (n = 3 biological replicates). *Error bars*: mean ± standard deviation. One-way ANOVA, **P* < .05, ***P* < .01, *****P* < .0001. (*E*) Caspase-3/7 activity assay of 8 patient-derived cIAP2 variants cotransfected with increasing doses of WT cIAP2 in HEK293T cells after TNF stimulation (n = 3 biological replicates). *Error bars*: mean ± SE. One-way ANOVA with multiple comparisons, ns (not significant) >.05, **P* < .05, ***P* < .01, ****P* < .001, *****P* < .0001. (*F*) Immunofluorescence assay of HeLa cells overexpressing cIAP2 variants and stimulated with TNF/BV6 for 6 hours. Quantitative analysis of cIAP2 (*green*) by fluorescence intensity in nucleus/cytoplasm. Blue: DAPI (4′,6-diamidino-2-phenylindole). *Scale bar*: 10 μm. Each data point represents a field (>2 cells per field, 25 fields in total; n = 3 biological replicates). *Error bars*: mean ± standard deviation. Two-way ANOVA. ***P* < .01, *****P* < .0001.

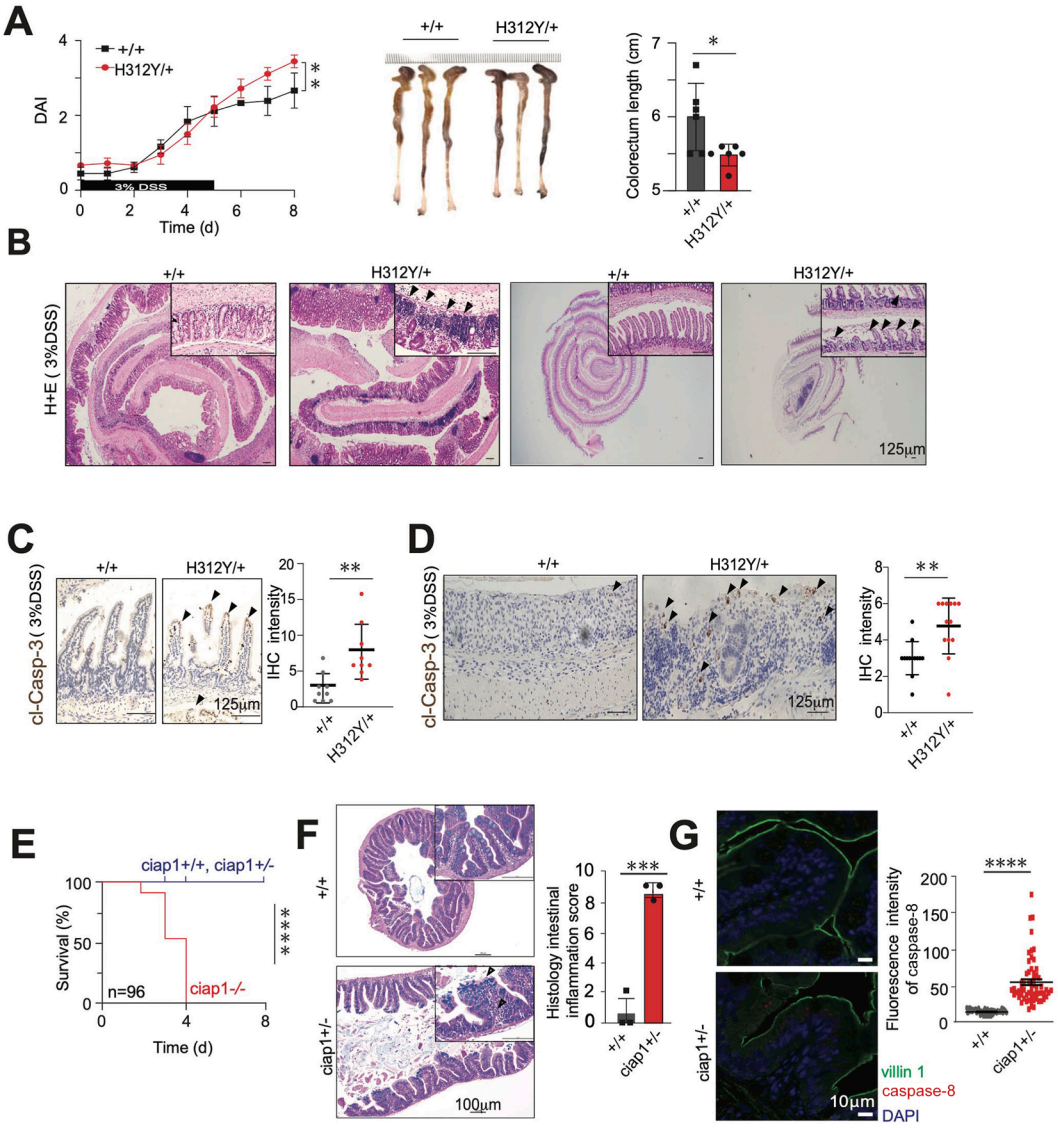
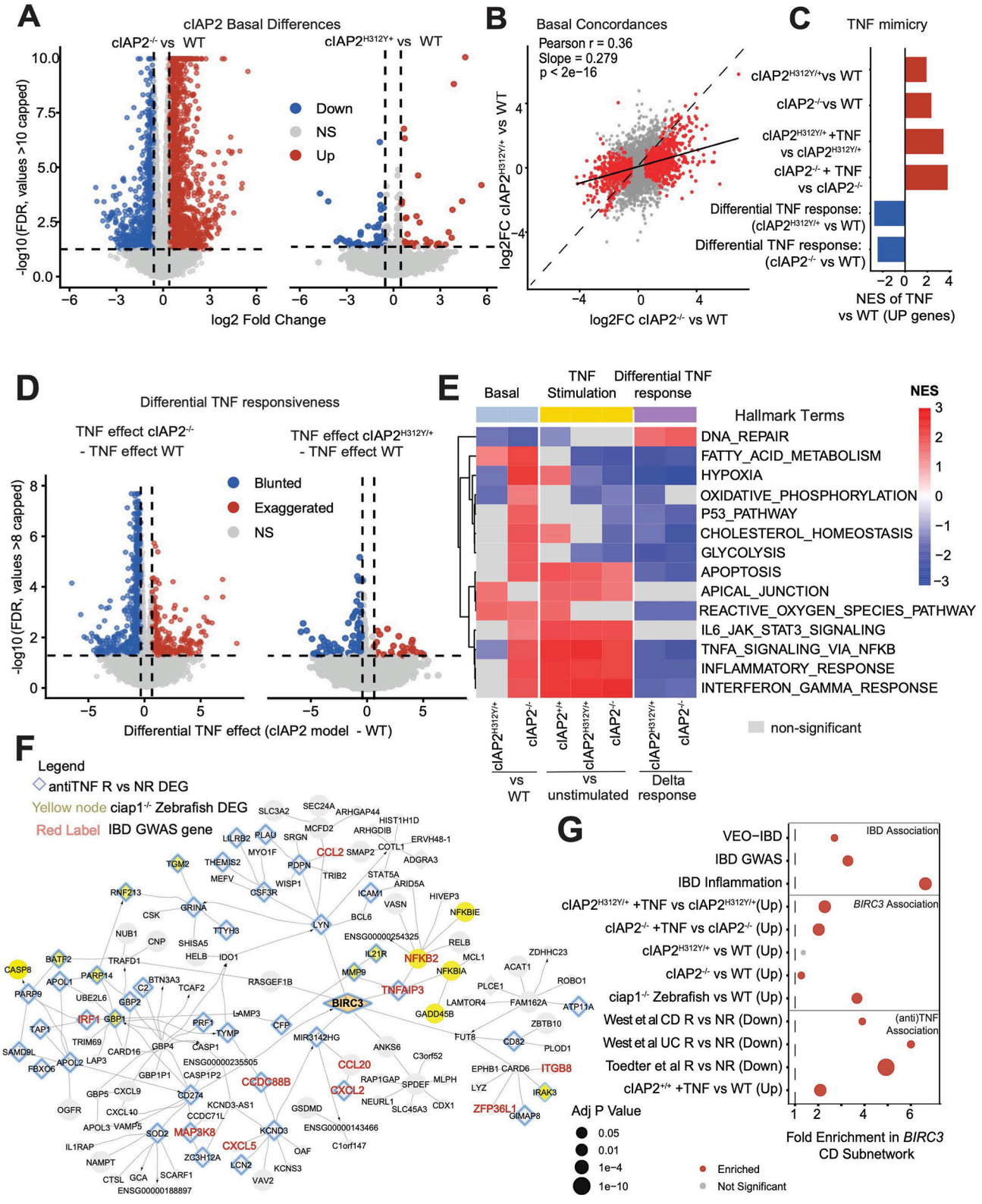


Figure 3. Animal studies of *BIRC3* deficiency. (*A*) Disease Activity Index (DAI) and gross morphology of cIAP2$^{+/+}$ and cIAP2$^{H312Y/+}$ mice. (*B*) Swiss-roll showing H&E-stained colon (*left 2 panels*) or small intestine (*right 2 panels*) sections. *Black arrows* indicate areas of inflammation. *Scale bar*: 125 μm. Immunohistochemistry of (*C*) small intestine and (*D*) colon showing cleaved caspase-3 (*black arrows*) in cIAP2$^{+/+}$ (n = 6) and cIAP2$^{H312Y/+}$ (n = 6) 3% DSS-treated mice. The immunohistochemistry (IHC) quantification was performed using 9 distinct fields of view per group. *Error bars*: mean ± standard error (SE). Unpaired *t* test, $^{**}P < .01$. (*E*) Kaplan-Meier survival curve of ciap1$^{+/+}$ (n = 25), ciap1$^{-/+}$ (n = 47), and ciap1$^{-/-}$ (n = 24) zebrafish (total n = 96). Log-rank Mantel-Cox test, $^{****}P < .0001$. (*F*) H&E-stained middle intestine sections of zebrafish at 1.5 years (n = 3). *Black arrows* indicate areas of inflammation. *Scale bar*: 100 μm. *Error bars*: mean ± SE. Unpaired *t* test, $^{***}P < .001$. (*G*) Immunofluorescence staining of adult zebrafish intestinal sections with caspase-8 (*red*), villin 1 (*green*), and 4′,6-diamidino-2-phenylindole (DAPI; *blue*). For each sample, 20 enterocytes were analyzed (n = 3). *Scale bar*: 10 μm. *Error bars*: mean ± SE. Two-tailed Welch's *t* test, $^{****}P < .0001$.

organoid findings and confirming that reduced or absent cIAP2 expression generates a gene expression signature closely resembling TNF stimulation (Supplementary Tables ST6 and 7).

Furthermore, the gene-level analysis revealed several candidate genes important in RIPK1-dependent cell death pathways, including the up-regulation of *casp8* in the ciap1$^{-/-}$ zebrafish; and the up-regulation (false discovery rate <0.05) of *Casp3, Nfkb2, Cflar* (encoding cFLIP) and *Tnfsf10* in the cIAP2$^{-/-}$ mice organoid model (Supplementary Tables ST1 and 7). Interestingly, we noted several metabolic pathways (eg, cholesterol homeostasis, fatty acid metabolism, and glycolysis) displayed altered baseline regulation in cIAP2$^{-/-}$ organoids with divergent responses upon TNF stimulation. Because these metabolic programs were not strongly induced by TNF in cIAP2$^{+/+}$ organoids, their basal activation represents a consequence of cIAP2$^{-/-}$ deficiency rather than TNF stimulation per se.

To understand the relevance of cIAP2 deficiency beyond Mendelian CD, we next contextualized *BIRC3* within regulatory programs active in adult CD. We leveraged a large Bayesian regulatory network constructed from mucosal


A
cIAP2 Basal Differences
cIAP2-/- vs WT
cIAP2H312Y+ vs WT
Down
NS
Up
-log10(FDR, values >10 capped)
log2 Fold Change
B
Basal Concordances
Pearson r = 0.36
Slope = 0.279
p < 2e−16
log2FC cIAP2H312Y/+ vs WT
log2FC cIAP2-/- vs WT
C
TNF mimicry
cIAP2H312Y/+vs WT
cIAP2-/-vs WT
cIAP2H312Y/+ +TNF vs cIAP2H312Y/+
cIAP2-/- + TNF vs cIAP2-/-
Differential TNF response: (cIAP2H312Y/+ vs WT)
Differential TNF response: (cIAP2-/- vs WT)
NES of TNF vs WT (UP genes)
D
Differential TNF responsiveness
TNF effect cIAP2-/- - TNF effect WT
TNF effect cIAP2H312Y/+ - TNF effect WT
Blunted
Exaggerated
NS
-log10 (FDR, values >8 capped)
Differential TNF effect (cIAP2 model - WT)
E
Basal
TNF Stimulation
Differential TNF response
Hallmark Terms
DNA_REPAIR
FATTY_ACID_METABOLISM
HYPOXIA
OXIDATIVE_PHOSPHORYLATION
P53_PATHWAY
CHOLESTEROL_HOMEOSTASIS
GLYCOLYSIS
APOPTOSIS
APICAL_JUNCTION
REACTIVE_OXYGEN_SPECIES_PATHWAY
IL6_JAK_STAT3_SIGNALING
TNFA_SIGNALING_VIA_NFKB
INFLAMMATORY_RESPONSE
INTERFERON_GAMMA_RESPONSE
NES
non-significant
cIAP2H312Y/+
cIAP2-/-
vs WT
vs unstimulated
Delta response
F
Legend
antiTNF R vs NR DEG
Yellow node ciap1-/- Zebrafish DEG
Red Label IBD GWAS gene
G
VEO−IBD
IBD GWAS
IBD Inflammation
cIAP2H312Y/+ +TNF vs cIAP2H312Y/+(Up)
cIAP2-/- +TNF vs cIAP2-/- (Up)
cIAP2H312Y/+ vs WT (Up)
cIAP2-/- vs WT (Up)
ciap1-/- Zebrafish vs WT (Up)
West et al CD R vs NR (Down)
West et al UC R vs NR (Down)
Toedter et al R vs NR (Down)
cIAP2+/+ +TNF vs WT (Up)
IBD Association
BIRC3 Association
(anti)TNF Association
Adj P Value
0.05
0.01
1e-4
1e-10
Enriched
Not Significant
Fold Enrichment in BIRC3 CD Subnetwork

transcriptomic profiles of ~400 adult CD patients representing both active and inactive disease states (Mount Sinai Crohn's and Colitis Registry cohort[37]). From this framework, we extracted a *BIRC3*-centered subnetwork encompassing regulatory interactions spanning up to 4 path lengths from *BIRC3*, yielding ~500 connected genes (Figure 4*F* and Supplementary Table ST8). This *BIRC3*-centric neighborhood was significantly enriched for multiple independent IBD-relevant gene signatures (Figure 4*G* and Supplementary Table ST9). These included genes up-regulated during active intestinal inflammation, genes located within IBD genome-wide association study,[31] and monogenic IBD genes.[32] Notably, the subnetwork was also enriched for transcriptional programs induced by *BIRC3* perturbation across cIAP2$^{-/-}$ model systems, including zebrafish and murine organoid models under basal and TNF-stimulated conditions, supporting the predicted *BIRC3* regulatory interactions in adult gut. Network topology revealed close connectivity of *BIRC3* with key inflammatory regulators, including *NFKB2* and its downstream effector *CCL20*, as well as central mediators of apoptosis and TNF signaling such as *TNFAIP3*.

Notably, the *BIRC3* subnetwork demonstrated strong enrichment for TNF-responsive gene programs and was significantly overrepresented among genes differentially expressed in anti-TNF nonresponders compared with responders across adult IBD cohorts.[33,34] To further evaluate the clinical relevance of this network, we calculated a GSVA score for the *BIRC3*-centered subnetwork in longitudinal mucosal biopsy samples from infliximab-treated patients in the ACT1 cohort.[34] At baseline, responders and nonresponders exhibited comparable subnetwork activity. However, by week 30 of infliximab therapy, responders demonstrated a significantly greater reduction in *BIRC3* mRNA as well as the *BIRC3* subnetwork GSVA score compared with nonresponders (Supplementary Figure S3 and Supplementary Table ST10). In contrast, nonresponders showed persistent subnetwork activation despite therapy.

Interestingly, the genotype interaction–associated programs largely mapped to metabolic and stress-response modules outside the immediate *BIRC3*-centered inflammatory subnetwork, suggesting *BIRC3* deficiency exerts dual effects. Overall, our findings support a model in which cIAP2 deficiency primes epithelial cells toward a constitutive inflammatory state and metabolically activated basal state while constraining dynamic responsiveness during a TNF challenge, revealing reduced signaling flexibility.

Figure 4. Integrative molecular analysis demonstrates the impact of reduced or absent *BIRC3* expression. (*A*) Basal transcriptional differences. Volcano plots showing differential gene expression in unstimulated cIAP2$^{-/-}$ and cIAP2$^{H312Y/+}$ mouse intestinal organoids compared with WT. cIAP2 deficiency induces a broad inflammatory transcriptional program at baseline, with a stronger magnitude in knockout (cIAP2$^{-/-}$) compared with heterozygous (cIAP2$^{H312Y/+}$) organoids. *Dashed vertical lines* denote log2 fold-change thresholds; *horizontal dashed lines* denote false discovery rate (FDR) cutoff. NS, not significant. (*B*) Basal concordance analysis. Genome-wide log2 fold changes (FC) between cIAP2$^{-/-}$ and cIAP2$^{H312Y/+}$ organoids demonstrated significant positive correlation (Pearson's $r = 0.36$, $P < 2\times10^{-16}$). Linear regression across all genes yielded a slope of 0.28, indicating that heterozygous organoids retain ~28% of the transcriptional amplitude observed in knockout organoids. Among genes significantly dysregulated in cIAP2$^{-/-}$ organoids (*red*), directional concordance was stronger ($r = 0.53$, $P < 2\times10^{-16}$), with a similar attenuation slope (~0.27). (*C*) TNF mimicry. Gene Set Enrichment Analysis using TNF-induced WT mouse organoid up-regulated (UP) genes demonstrates that cIAP2$^{-/-}$ and cIAP2$^{H312Y/+}$ mouse organoids both partially recapitulate TNF-responsive programs in the absence of stimulation. Positive (*red*) normalized enrichment scores (NES) indicate constitutive activation of TNF-associated pathways, whereas interaction terms, indicating differential TNF response and defined as TNF effect in cIAP2 model vs TNF effect in control organoids, show attenuation (*blue*) relative to WT. Ranking metric was the *t* statistic and all assessments an FDR <0.05 (Supplementary Table ST4). (*D*) Differential TNF responsiveness (interaction analysis). Volcano plots depict the interaction term, or differential TNF response, defined as the change in TNF response in mutant organoids relative to WT (ie, ΔTNF_mutant—ΔTNF_WT). Both models show a predominantly blunted TNF response (*blue coloring*), indicating impaired dynamic adaptation to TNF stimulation. (*E*) Hallmark pathway analysis. Heat map of hallmark gene set enrichment analysis (GSEA) across basal, TNF-stimulated (+TNF or −TNF), and interaction (genotype: TNF) conditions. A subset of pathways is shown with intensity and coloring representing positive (*red*) or negative (*blue*) NES. Ranking statistic was the *t* statistic, and only significant pathway terms show NES, with *grey* coloring indicating nonsignificant enrichment. Full results in Supplementary Table ST5. Note negative NES for differential TNF response gene rankings indicates pathways that are attenuated or amplified. IL, interleukin; JAK, Janus kinase; NFKB, nuclear factor-κB; STAT3, signal transducer and activator of transcription 3. (*F*) A *BIRC3*-centric gene regulatory subnetwork was generated by querying *BIRC3* plus 4 path lengths in a Bayesian network of ~8000 genes generated using transcriptional profiles of colonic biopsy specimens from a cohort of adult CD patients. Nodes are colored *yellow* if the gene was identified as differentially expressed in the ciap$^{-/-}$ zebrafish model and are outlined in *blue* if identified as a gene reported as differentially expressed between anti-TNF responders and nonresponders (NR). *Red* text coloring indicates an IBD genome-wide association study (GWAS) gene. Edges are directed and represent statistically inferred causal regulatory relationships. (*G*) The fold enrichment for the overlap between various gene sets and the *BIRC3* centric subnetwork genes described in *C*. Size of *dots* represents the level of significance (as log10 Benjamini-Hochberg–adjusted Fisher's exact test *P* value). Gene sets are categorized according to their informing on IBD association (where IBD Inf = DEGs in inflamed vs uninflamed human IBD mucosa samples); IBD GWAS and known very early-onset (VEO) IBD genes; or cIAP2 association (DEGs from various cIAP perturbation models) and anti-TNF association (DEGs from cIAP2$^{+/+}$ TNF vs cIAP2$^{+/+}$ and published gene sets associated with anti-TNF response in ulcerative colitis [UC] and CD).

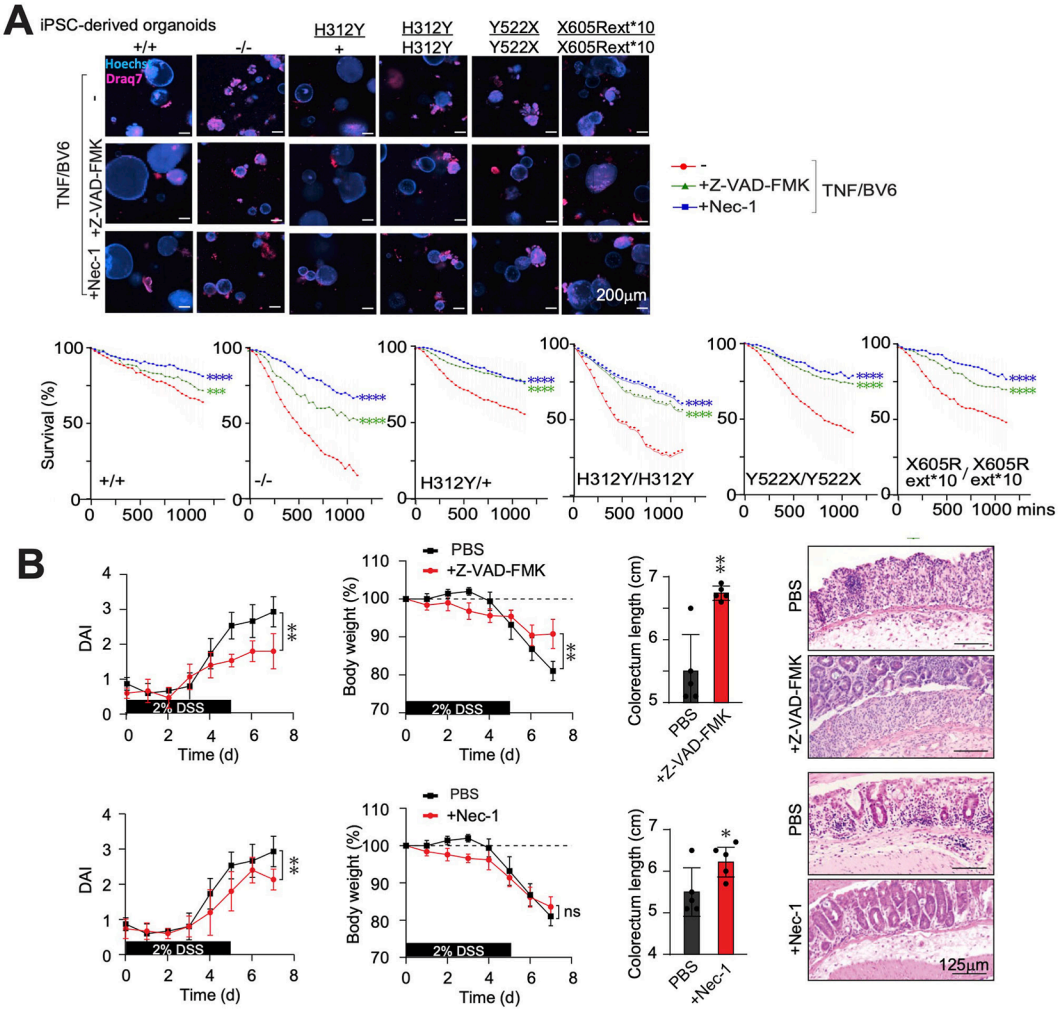


Figure 5. Treatment of *BIRC3* deficiency. (*A*) Live-cell immunofluorescence assay and quantitative analysis of TNF/BV6-induced cell death in human iPSC-derived intestinal organoids, and the effects of Z-VAD-FMK and Nec-1 rescue. *Blue*: Hoechst; *Red*: Draq7. *Scale bar*: 200 μm (n = 4 biological replicates). *Error bars*: mean ± standard deviation. Two-way analysis of variance, ****$P < .0001$. (*B*) Mice were treated with 5 days of 2% DSS and 3 days of water received phosphate buffered saline (PBS) (n = 5), Z-VAD-FMK (3 mg/kg) (n = 5) (*top*), or Nec-1 (1.5 mg/kg) (n = 5) (*bottom*). Measurements included body weight change, Disease Activity Index (DAI), colon length change, and H&E staining. *Scale bar*: 125 μm. Statistical analyses were performed at the predefined experimental end point. *Error bars*: mean ± standard error. Unpaired *t* test, not significant (ns) $P > .05$, *$P < .05$, **$P < .01$.

Pharmacologic Inhibition of RIPK1 and Caspases Attenuates Inflammation and Cell Death in cIAP2-Deficient Models

To explore potential therapeutic strategies for patients with dysregulated cIAP2-associated CD, we tested for enrichment in molecular signatures of birinapant,[44] a SMAC mimetics targeting cIAP1/2 and X-linked inhibitor of apoptosis protein (XIAP) used in clinical cancer trials, and necrostatin 1[45] (Nec-1), a small-molecule RIPK1 inhibitor, curated from the LINCS L1000 chemical perturbation consensus database.[46] The gene signatures induced by birinapant closely resembled the transcriptional effects observed in ciap1-deficient zebrafish and cIAP2-deficient mouse organoids. In contrast, gene expression signatures induced by Nec-1 treatment were significantly enriched among DEGs from cIAP2-knockout models but largely in the opposing direction, suggesting a potential therapeutic target for these patients with *BIRC3* variants (Supplementary Table ST11).

Live-cell imaging of human iPSC-derived intestinal organoids revealed increased cell death with either cIAP2 knockout ($cIAP2^{-/-}$) or knock-in of several patient cIAP2 variants after treatment with TNF and the SMAC mimetic BV6 compared with WT controls. However, treatment with Z-VAD-FMK,[47] a pan-caspase inhibitor, or Nec-1 markedly reduced the Draq7 signal, indicating that both inhibitors conferred protection against TNF-induced cell death (Figure 5*A*). Similar protective effects were seen in HCT116 cells with cIAP2 knockout or lentiviral knock-in overexpression of several patient variants (Supplementary Figure S4).

Finally, we evaluated these potential therapeutic small molecule inhibitors using our $cIAP2^{H312Y/+}$ mouse model.

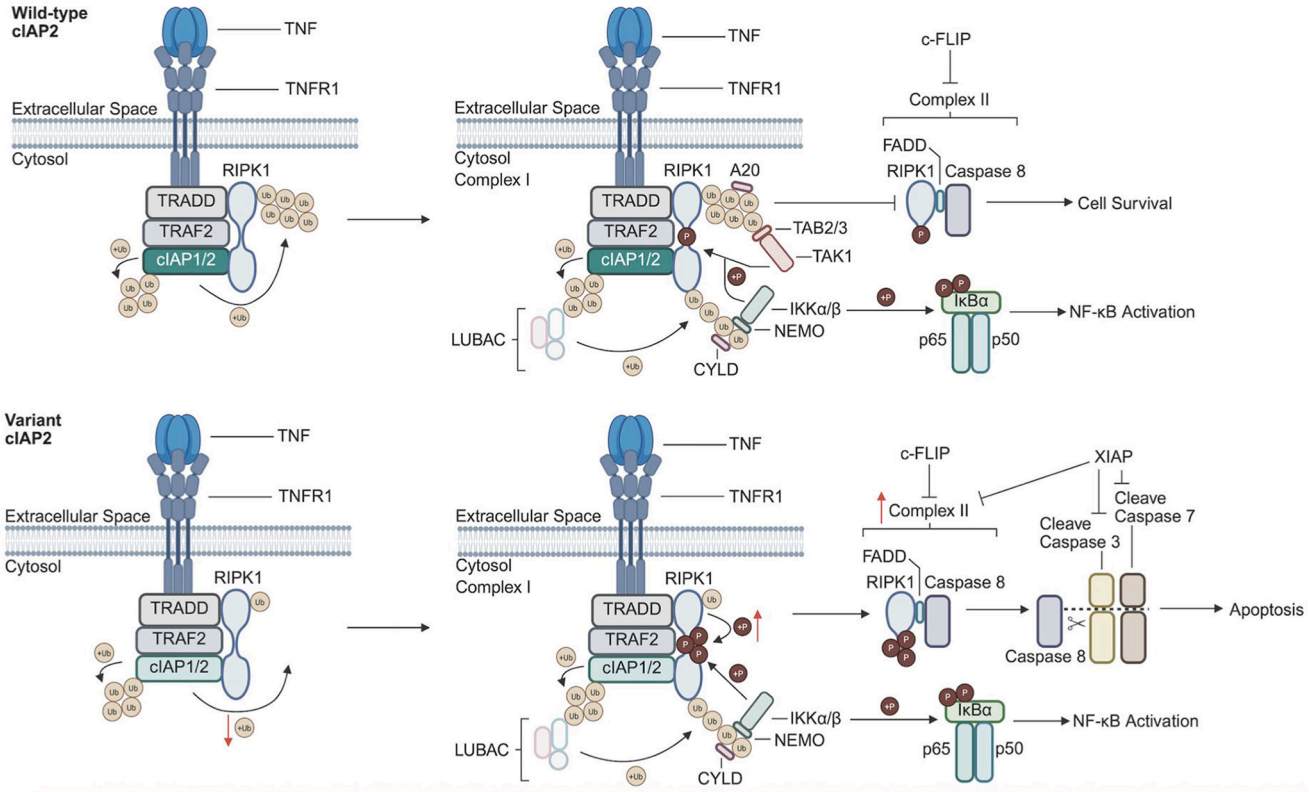


Figure 6. cIAP2 signaling pathway. Schematic model illustrates cIAP2 signaling. WT cIAP2 enhances TNF-induced RIPK1 ubiquitination while limiting its phosphorylation, thereby suppressing the formation of active complex II and promoting cell survival. In contrast, cIAP2 variants fail to regulate RIPK1 ubiquitination, which leads to increased autophosphorylation. As a result, active complex II will further cleave caspases 3 and 7, leading to cell apoptosis. c-FLIP, cellular FADD-like IL-1β–converting enzyme-inhibitory protein; FADD, FAS-associated death domain protein; IKKα/β, IκB kinase; LUBAC, linear ubiquitin chain assembly complex; NEMO, nuclear factor-κB essential modulator; NF-κB, nuclear factor-κB; TAK1, transforming growth factor-β–activated kinase 1; TNFR1, TNF receptor 1; TRADD, TNFRSF1A associated via death domain; TRAF2, TNF receptor-associated factor 2; XIAP, X-linked inhibitor of apoptosis protein.

Intraperitoneal injection of Z-VAD-FMK or Nec-1 reduced colonic inflammation in DSS-treated cIAP2$^{H312Y/+}$ mice, as indicated by reduced Disease Activity Index and improved histopathology compared with untreated cIAP2$^{H312Y/+}$ mice littermates (Figure 5*B*).

Discussion

We describe 8 germline *BIRC3* genetic variants identified in 14 people with CD from 10 families diagnosed between infancy and adulthood and presenting with typical features of colonic or Ileocolonic CD. Knock-in cIAP2$^{H312Y/+}$ mice and heterozygote ciap1$^{-/+}$ zebrafish recapitulated key features of the human intestinal phenotype, including intestinal inflammation with epithelial apoptosis. The experimental and molecular data demonstrate that all 8 *BIRC3* genetic variants resulted in reduced cIAP2 protein function that could be rescued by WT cIAP2 (mechanism is outlined in Figure 6). Another important finding is that identified *BIRC3* variants were either autosomal dominant (AD) or autosomal recessive (AR), indicating mixed inheritance. As expected, the AR variants (3 independent consanguineous families harbored homozygous cIAP2 variants (p.Y522X, p.C588Y, and p.X605Rext*10) resulted in a stronger phenotype with early diagnosis of CD (infancy) and several extra-intestinal manifestation of disease, including fever, skin, and joint inflammation, whereas the AD variants presented as older children and adults with typical CD features. Therefore, we believe the AR and AD inheritance strengthens the findings and suggests a broader role of cIAP2 in CD pathogenesis.

However, with the wide age range of disease onset, even within families, the identification of additional CD patients with *BIRC3* variants and complete familial genotyping is required to determine the disease penetrance and whether there is variable expressivity in CD phenotypes. Similarly, variants in several genes involved in regulating TNF signaling, including *NFKB1*,[48] *RelA*,[49] *OTULIN*,[50] and *TNFAIP3*/A20[51] result in haploinsufficiency, and *OTULIN*-deficiency[50] has both an AR and AD mixed inheritance pattern similar to what we describe here for *BIRC3*. Moreover, incomplete penetrance and variable expressivity is commonly described in patients with both monoallelic and biallelic TNF-signaling defects (reviewed by Lalaoui and Masters[52]).

Although 8 patients from 7 independent families had missense *BIRC3* variants, 6 patients from 3 independent families had *BIRC3* variants that resulted in premature termination codons. Two of the 3 *BIRC3* premature termination codon variants were located in the final exon, and 1 premature termination codon variant was in the penultimate exon less than 50 nucleotides upstream from the exon-exon junction; therefore, these transcripts would be expected to escape nonsense mediated decay[53] and express truncated cIAP2 proteins.

As we have shown here, these truncated proteins cause reduced but not complete loss of cIAP2 protein function. Multisystem transcriptomic analyses reveal that cIAP2 functions as a dosage-sensitive regulator of TNF signaling, shaping inflammatory activation, metabolic adaptation, and epithelial survival. This integrative framework links *BIRC3*-deficiency to both Mendelian intestinal disease and broader TNF-dependent inflammatory pathways in human IBD.

BIRC3 deficiency results in CD without the significant immunodeficiency and systemic disease that is associated with other TNF-signaling defects, suggesting a specific role for cIAP2 in the intestinal epithelium homeostasis. Mechanistically, the patient-derived cIAP2 variants impaired RIPK1 ubiquitylation, resulting in increased RIPK1 autophosphorylation and cell death upon challenge with TNF. RNA-seq analysis demonstrated that reduced cIAP2 resulted in constitutive activation of TNF signaling pathways and a blunted response to TNF stimulation. Furthermore, the patient-derived cIAP2 variants increased the expression of *CCL5* and *CCL20* chemokines, suggesting that cIAP2-deficiency may also lead to the infiltration of immune cells into the intestine. Coenrichment of *BIRC3* with TNF responder vs nonresponder genes in the adult CD subnetwork suggested a broader relevance of *BIRC3* expression beyond Mendelian disease in polygenic CD. Although cIAP1 and cIAP2 both have putative roles in mediating TNF signaling (reviewed by Zeissig and Petersen[11] and Lalaoui and Vaux DL[12]), we demonstrate that in intestinal epithelium, cIAP2 has a distinct role in regulating TNF response.

Whereas our studies primarily focused on the role of cIAP2 in maintaining intestinal homeostasis, it is possible that nonepithelial cells, including immune cells, as well as other nonapoptotic cellular pathways contribute to disease pathogenesis. Previous studies have demonstrated that enzymatically inactive cIAP1/2 mice died during embryonic development due to dysregulated RIPK1-mediated apoptosis[14] and that cIAP2-deficient mice exhibit increased susceptibility to chemically induced colitis.[15,16] The cIAP1$^{-/-}$ mice with inducible knockout of cIAP2 die within 3 days, exhibiting overt inflammation and apoptosis in the intestine and liver, primarily driven by caspase-8.[54] Together, this implies complex regulation of cIAP1 and cIAP2 and that further study of cIAP2 regulation, specifically in human disease, will provide insight into not only the immune regulation of inflammation but also CD pathogenesis.

Conventional IBD treatment strategies often fail to achieve sustained remission, highlighting the need for targeted therapeutic approaches, and yet, there is still no molecular rationale for the selection of specific biologics or small molecules. Our study reveals an essential and protective role of cIAP2 in regulating TNF-mediated cell death and intestinal injury. Dysregulation of TNF-responsive gene expression in polygenic CD, suggests that modulating pathways disrupted by loss of cIAP2 could offer new therapeutic strategies for CD patients. To this point, we showed the therapeutic potential of a pan-caspase inhibitor (Z-VAD-FMK) and RIPK1 inhibitor (Nec-1) in human iPSC-derived intestinal organoids. Furthermore, the administration of these inhibitors in the cIAP2$^{H312Y/+}$ mouse model successfully alleviated key pathologic features associated with CD in patients, including intestinal inflammation, epithelial cell damage, and crypt loss.

Of note, the RIPK1 inhibitor GSK2982772, a Nec-1 analogue, has been evaluated in patients with active ulcerative colitis.[55–57] GSK2982772 was generally well-tolerated by patients but did not significantly outperform the placebo. Nevertheless, our study, along with GSK2982772 and ongoing RIPK1 inhibitor clinical trials, including GDC-8264[58] and others (ABBV-668 and SAR443122 reviewed by Vieujean et al[17]), suggests that RIPK1 is a promising IBD molecular target and stratifying patients (eg, CD and/or dysregulated TNF signaling) may improve therapeutic outcomes.

These results highlight the therapeutic potential of targeting dysregulated cell death pathways through small molecule inhibition of RIPK1 in patients with *BIRC3* deficiency, other TNF-related forms of monogenic CD, and potentially in a subset of polygenic CD characterized by identifying similar transcriptional profiles.

Supplementary Material

Note: To access the supplementary material accompanying this article, visit the online version of *Gastroenterology* at www.gastrojournal.org, and at https://doi.org/10.1053/j.gastro.2026.05.022.

References

1. **Hracs L, Windsor JW,** Gorospe J, et al. Global evolution of inflammatory bowel disease across epidemiologic stages. Nature 2025;642:458–466.
2. Crowley E, Warner N, Pan J, et al. Prevalence and clinical features of inflammatory bowel diseases associated with monogenic variants, identified by whole-exome sequencing in 1000 children at a single center. Gastroenterology 2020;158:2208–2220.
3. Nambu R, Warner N, Mulder DJ, et al. A systematic review of monogenic inflammatory bowel disease. Clin Gastroenterol Hepatol 2022;20:e653–e663.
4. **Gaibee Z, Warner N, Bugda**, et al. The genetic architecture of congenital diarrhea and enteropathy. N Engl J Med 2025;392:1297–1309.
5. **Li Y, Fuhrer M, Bahrami E**, et al. Human RIPK1 deficiency causes combined immunodeficiency and inflammatory bowel diseases. Proc Natl Acad Sci U S A 2019;116:970–975.

6. **Tao P, Sun J, Wu Z**, et al. A dominant autoinflammatory disease caused by non-cleavable variants of RIPK1. Nature 2020;577:109–114.
7. **Cuchet-Lourenco D, Eletto D, Wu C**, et al. Biallelic RIPK1 mutations in humans cause severe immunodeficiency, arthritis, and intestinal inflammation. Science 2018;361:810–813.
8. Lehle AS, Farin HF, Marquardt B, et al. Intestinal inflammation and dysregulated immunity in patients with inherited caspase-8 deficiency. Gastroenterology 2019; 156:275–278.
9. Zilberman-Rudenko J, Shawver LM, Wessel AW, et al. Recruitment of A20 by the C-terminal domain of NEMO suppresses NF-κB activation and autoinflammatory disease. Proc Natl Acad Sci U S A 2016;113:1612–1617.
10. **Zeissig Y, Petersen BS,** Milutinovic S, et al. XIAP variants in male Crohn's disease. Gut 2015;64:66–76.
11. Lalaoui N, Vaux DL. Recent advances in understanding inhibitor of apoptosis proteins. F1000Res 2018;7. F1000 Faculty Rev-1889.
12. Darding M, Meier P. IAPs: guardians of RIPK1. Cell Death Differ 2012;19:58–66.
13. **Conte D, Holcik M,** Lefebvre CA, et al. Inhibitor of apoptosis protein cIAP2 is essential for lipopolysaccharide-induced macrophage survival. Mol Cell Biol 2006;26:699–708.
14. **Schorn F, Werthenbach JP**, Hoffmann M, et al. cIAPs control RIPK1 kinase activity-dependent and-independent cell death and tissue inflammation. EMBO J 2023; 42:e113614.
15. Dagenais M, Dupaul-Chicoine J, Champagne C, et al. A critical role for cellular inhibitor of protein 2 (cIAP2) in colitis-associated colorectal cancer and intestinal homeostasis mediated by the inflammasome and survival pathways. Mucosal Immunol 2016;9:146–158.
16. **Bertrand MJ, Doiron K**, Labbe K, et al. Cellular inhibitors of apoptosis cIAP1 and cIAP2 are required for innate immunity signaling by the pattern recognition receptors NOD1 and NOD2. Immunity 2009;30:789–801.
17. Vieujean S, Jairath V, Peyrin-Biroulet L, et al. Understanding the therapeutic toolkit for inflammatory bowel disease. Nat Rev Gastroenterol Hepatol 2025;22:371–394.
18. Yao Y, Kim G, Shafer S, et al. Mucus sialylation determines intestinal host-commensal homeostasis. Cell 2022;185:1172–1188.e28.
19. Uhlig HH, Booth C, Cho J, et al. Precision medicine in monogenic inflammatory bowel disease: proposed mIBD REPORT standards. Nat Rev Gastroenterol Hepatol 2023;20:810–828.
20. Jardine S, Anderson S, Babcock S, et al. Drug screen identifies leflunomide for treatment of inflammatory bowel disease caused by TTC7A deficiency. Gastroenterology 2020;158:1000–1015.
21. **Wang L, Aschenbrenner D, Zeng Z**, et al. Gain-of-function variants in SYK cause immune dysregulation and systemic inflammation in humans and mice. Nat Genet 2021;53:500–510.
22. **Li D, Qiu Z,** Shao Y, et al. Heritable gene targeting in the mouse and rat using a CRISPR-Cas system. Nat Biotechnol 2013;31:681–683.
23. **Shao Y, Guan Y, Wang L**, et al. CRISPR/Cas-mediated genome editing in the rat via direct injection of one-cell embryos. Nat Protoc 2014;9:2493–2512.
24. **Montague TG, Cruz JM**, Gagnon JA, et al. CHOP-CHOP: a CRISPR/Cas9 and TALEN web tool for genome editing. Nucleic Acids Res 2014;42:W401–W407.
25. Robinson MD, Oshlack A. A scaling normalization method for differential expression analysis of RNA-seq data. Genome Biol 2010;11:R25.
26. Ritchie ME, Phipson B, Wu D, et al. limma powers differential expression analyses for RNA-sequencing and microarray studies. Nucleic Acids Res 2015;43:e47.
27. Law CW, Chen Y, Shi W, et al. voom: precision weights unlock linear model analysis tools for RNA-seq read counts. Genome Biol 2014;15:R29.
28. **Suarez-Farinas M, Tokuyama M**, Wei G, et al. Intestinal inflammation modulates the expression of ACE2 and TMPRSS2 and potentially overlaps with the pathogenesis of SARS-CoV-2-related disease. Gastroenterology 2021;160:287–301.e20.
29. Hu Y, Flockhart I, Vinayagam A, et al. An integrative approach to ortholog prediction for disease-focused and other functional studies. BMC Bioinformatics 2011;12:357.
30. **Subramanian A, Tamayo P, Mootha VK**, et al. Gene set enrichment analysis: a knowledge-based approach for interpreting genome-wide expression profiles. Proc Natl Acad Sci U S A 2005;102:15545–15550.
31. **de Lange KM, Moutsianas L, Lee JC**, et al. Genome-wide association study implicates immune activation of multiple integrin genes in inflammatory bowel disease. Nat Genet 2017;49:256–261.
32. **Bolton C, Smillie CS**, Pandey S, et al. An integrated taxonomy for monogenic inflammatory bowel disease. Gastroenterology 2022;162:859–876.
33. **West NR, Hegazy AN**, Owens BMJ, et al. Oncostatin M drives intestinal inflammation and predicts response to tumor necrosis factor-neutralizing therapy in patients with inflammatory bowel disease. Nat Med 2017; 23:579–589.
34. **Toedter G, Li K, Marano C**, et al. Gene expression profiling and response signatures associated with differential responses to infliximab treatment in ulcerative colitis. Am J Gastroenterol 2011;106:1272–1280.
35. Wickham H. ggplot2: Elegant Graphics for Data Analysis. Use R! 2nd ed. Cham: Springer International Publishing: Imprint: Springer, 2016.
36. Peters LA, Perrigoue J, Mortha A, et al. A functional genomics predictive network model identifies regulators of inflammatory bowel disease. Nat Genet 2017; 49:1437–1449.
37. **Argmann C, Hou R**, Ungaro RC, et al. Biopsy and blood-based molecular biomarker of inflammation in IBD. Gut 2023;72:1271–1287.
38. Zhu J, Zhang B, Smith EN, et al. Integrating large-scale functional genomic data to dissect the complexity of yeast regulatory networks. Nat Genet 2008;40:854–861.
39. Shannon P, Markiel A, Ozier O, et al. Cytoscape: a software environment for integrated models of biomolecular interaction networks. Genome Res 2003; 13:2498–2504.

40. Karczewski KJ, Francioli LC, Tiao G, et al. The mutational constraint spectrum quantified from variation in 141,456 humans. Nature 2020;581:434–443.
41. Rentzsch P, Witten D, Cooper GM, et al. CADD: predicting the deleteriousness of variants throughout the human genome. Nucleic Acids Res 2019;47:D886–D894.
42. Richards S, Aziz N, Bale S, et al. Standards and guidelines for the interpretation of sequence variants: a joint consensus recommendation of the American College of Medical Genetics and Genomics and the Association for Molecular Pathology. Genet Med 2015; 17:405–424.
43. Santoro MM, Samuel T, Mitchell T, et al. Birc2 (clap1) regulates endothelial cell integrity and blood vessel homeostasis. Nat Genet 2007;39:1397–1402.
44. Krepler C, Chunduru SK, Halloran MB, et al. The novel SMAC mimetic birinapant exhibits potent activity against human melanoma cells. Clin Cancer Res 2013; 19:1784–1794.
45. Degterev A, Huang Z, Boyce M, et al. Chemical inhibitor of nonapoptotic cell death with therapeutic potential for ischemic brain injury. Nat Chem Biol 2005;1:112–119.
46. **Evangelista JE, Clarke DJB, Xie Z**, et al. SigCom LINCS: data and metadata search engine for a million gene expression signatures. Nucleic Acids Res 2022; 50:W697–W709.
47. Zhu H, Fearnhead HO, Cohen GM. An ICE-like protease is a common mediator of apoptosis induced by diverse stimuli in human monocytic THP.1 cells. FEBS Lett 1995; 374:303–308.
48. Lorenzini T, Fliegauf M, Klammer N, et al. Characterization of the clinical and immunologic phenotype and management of 157 individuals with 56 distinct heterozygous NFKB1 mutations. J Allergy Clin Immunol 2020; 146:901–911.
49. **Badran YR, Dedeoglu F**, Leyva Castillo JM, et al. Human RELA haploinsufficiency results in autosomal-dominant chronic mucocutaneous ulceration. J Exp Med 2017;214:1937–1947.
50. **Davidson S, Shibata Y,** Collard S, et al. Dominant negative OTULIN-related autoinflammatory syndrome. J Exp Med 2024;221:e20222171.
51. **Zhou Q, Wang H,** Schwartz DM, et al. Loss-of-function mutations in TNFAIP3 leading to A20 haploinsufficiency cause an early-onset autoinflammatory disease. Nat Genet 2016;48:67–73.
52. Lalaoui N, Masters SL. Monogenic disorders of the TNF signalling pathway. Nat Rev Rheumatol 2026;22:8–25.
53. Mendell JT, Sharifi NA, Meyers JL, et al. Nonsense surveillance regulates expression of diverse classes of mammalian transcripts and mutes genomic noise. Nat Genet 2004;36:1073–1078.
54. Zhang J, Webster JD, Dugger DL, et al. Ubiquitin ligases cIAP1 and cIAP2 limit cell death to prevent inflammation. Cell Rep 2019;27:2679–2689.e3.
55. Weisel K, Scott N, Berger S, et al. A randomised, placebo-controlled study of RIPK1 inhibitor GSK2982772 in patients with active ulcerative colitis. BMJ Open Gastroenterol 2021;8:e000680.
56. Weisel K, Scott NE, Tompson DJ, et al. Randomized clinical study of safety, pharmacokinetics, and pharmacodynamics of RIPK1 inhibitor GSK2982772 in healthy volunteers. Pharmacol Res Perspect 2017;5:e00365.
57. Harris PA, Berger SB, Jeong JU, et al. Discovery of a first-in-class receptor interacting protein 1 (RIP1) kinase specific clinical candidate (GSK2982772) for the treatment of inflammatory diseases. J Med Chem 2017; 60:1247–1261.
58. Jones NS, Kshirsagar S, Mohanan V, et al. A phase I, randomized, ascending-dose study to assess safety, pharmacokinetics, and activity of GDC-8264, a RIP1 inhibitor, in healthy volunteers. Clin Transl Sci 2023; 16:1997–2009.

Author names in bold designate shared co-first authorship.

Received October 24, 2025. Accepted May 26, 2026.

Correspondence
Address correspondence to: Aleixo M. Muise, MD, PhD, The Hospital for Sick Children, 555 University Avenue, Toronto, Ontario M5G 1X8, Canada. e-mail: aleixo.muise@utoronto.ca; or Dali Li, PhD, Shanghai Frontiers Science Center of Genome Editing and Cell Therapy, Shanghai Key Laboratory of Regulatory Biology, School of Life Sciences, East China Normal University, No. 500 Dongchuan Road, Minhang District, Shanghai 200241, China. e-mail: dlli@bio.ecnu.edu.cn; or Daniel Kotlarz, MD, PhD, Dr. von Hauner Children's Hospital, Department of Pediatrics, University Hospital, Ludwig Maximilian University Munich, Lindwurmstraße 4, 80337, Munich, Germany. e-mail: daniel.kotlarz@med.uni-muenchen.de.

Acknowledgments
The authors thank all of the patients and their families for participating in this study and the coordinators as part of the Very Early Onset Inflammatory Bowel Disease (VEO-IBD) Consortium (www.VEOIBD.org). The generation of zebrafish *birc2* mutant lines and genotyping was performed by Xiucheng Cui and Jason Burgess in Zebrafish Genetics and Disease Models Facility, The Hospital for Sick Children, Toronto, Ontario, Canada. Yue Li has provided expertise in immunophenotyping of patients with BIRC3 deficiency.

CRediT Authorship Contributions
Qi Li, PhD (Conceptualization: Supporting; Formal analysis: Equal; Writing – original draft: Supporting; Writing – review & editing: Supporting)
Ryusuke Nambu, MD (Conceptualization: Equal; Formal analysis: Equal; Writing – original draft: Equal; Writing – review & editing: Equal)
Hu Yaqiang, PhD (Formal analysis: Equal; Writing – original draft: Equal; Writing – review & editing: Equal)
Xiang Shen, MSc (Conceptualization: Supporting; Formal analysis: Equal; Writing – original draft: Equal; Writing – review & editing: Equal)
Carmen Argmann, PhD (Conceptualization: Equal; Data curation: Equal; Formal analysis: Equal; Writing – original draft: Equal; Writing – review & editing: Equal)
Rei Guan, PhD (Formal analysis: Equal; Writing – original draft: Equal; Writing – review & editing: Equal)
Erin Janssen, MD, PhD (Conceptualization: Equal; Data curation: Equal; Formal analysis: Equal; Writing – original draft: Equal; Writing – review & editing: Equal)
Tom Le Voyer, MD, PhD (Conceptualization: Equal; Formal analysis: Equal; Writing – review & editing: Equal)
Neil Warner, PhD (Data curation: Supporting; Formal analysis: Supporting; Writing – original draft: Supporting; Writing – review & editing: Supporting)
Daniel D. Yu, MSc (Formal analysis: Supporting; Writing – review & editing: Supporting)
Jing Guo, MD (Validation: Supporting; Writing – review & editing: Supporting)
Kelvin Long, BSc (Formal analysis: Supporting; Writing – review & editing: Supporting)
Jodie Ouahed, MD, PhD (Formal analysis: Supporting; Writing – review & editing: Supporting)
Michael Field, PhD (Formal analysis: Supporting; Writing – review & editing: Supporting)
Lauren Collen, MD (Formal analysis: Supporting; Writing – review & editing: Supporting)
Jonas Bibus, MSc (Formal analysis: Supporting; Writing – review & editing: Supporting)
David Illig, PhD (Formal analysis: Supporting; Writing – review & editing: Supporting)

Meino Rohlfs, PhD (Formal analysis: Supporting; Writing – review & editing: Supporting)
Ziqi Yu, MSc (Formal analysis: Supporting; Writing – review & editing: Supporting)
Shaohong Yang, MD (Formal analysis: Supporting; Writing – review & editing: Supporting)
Wenjuan Li, PhD (Formal analysis: Supporting; Writing – review & editing: Supporting)
Craig D. Platt, MD, PhD (Formal analysis: Supporting; Writing – review & editing: Supporting)
Phillip H. Comella, PhD (Formal analysis: Supporting; Writing – review & editing: Supporting)
Daniel Jordan, PhD (Formal analysis: Supporting; Writing – review & editing: Supporting)
Mayte Suárez-Fariñas, PhD (Formal analysis: Supporting; Writing – review & editing: Supporting)
Mohammed F. Alosaimi, MD (Formal analysis: Supporting; Writing – review & editing: Supporting)
Lauren A. Peters, PhD (Formal analysis: Supporting; Writing – review & editing: Supporting)
Jeremie Rosain, PhD (Formal analysis: Supporting; Writing – review & editing: Supporting)
Claire Fieschi, MD, PhD (Formal analysis: Supporting; Writing – review & editing: Supporting)
Anne Puel, PhD (Supervision: Supporting; Writing – review & editing: Supporting)
Elena W.Y. Hsieh, MD (Formal analysis: Supporting; Writing – review & editing: Supporting)
Takeo Naito, MD PhD (Formal analysis: Supporting; Writing – review & editing: Supporting)
Zhiyang Zeng, PhD (Formal analysis: Supporting; Writing – review & editing: Supporting)
Marta Velasco Rodríguez-Belvís, MD (Formal analysis: Supporting; Writing – review & editing: Supporting)
Laura Palomino, MD (Formal analysis: Supporting; Writing – review & editing: Supporting)
Peter Küster, MD (Formal analysis: Supporting; Writing – review & editing: Supporting)
Dalin Li, PhD (Formal analysis: Supporting; Writing – review & editing: Supporting)
Christoph Klein, MD, PhD (Funding acquisition: Supporting; Supervision: Supporting; Writing – review & editing: Supporting)
Scott B. Snapper, MD, PhD (Funding acquisition: Supporting; Supervision: Supporting; Writing – review & editing: Supporting)
Jean-Laurent Cassanova, MD, PhD (Supervision: Supporting; Writing – review & editing: Supporting)
Raif Geha, MD (Supervision: Supporting; Writing – original draft: Supporting; Writing – review & editing: Supporting)
Edward Hoffenberg, MD (Formal analysis: Supporting; Writing – review & editing: Supporting)
Dermot P.B. McGovern, MD, PhD (Funding acquisition: Supporting; Supervision: Equal; Writing – original draft: Equal; Writing – review & editing: Equal)
Eric Schadt, PhD (Funding acquisition: Supporting; Supervision: Equal; Writing – original draft: Equal; Writing – review & editing: Equal)
Daniel Kotlarz, MD, PhD (Conceptualization: Lead; Funding Acquisition: Equal; Methodology: Equal; Supervision: Equal; Writing – original draft: Equal; Writing – review & editing: Equal)
Dali Li, PhD (Methodology: Equal; Supervision: Equal; Writing – original draft: Equal; Writing – review & editing: Equal)
Aleixo M. Muise, MD, PhD (Conceptualization: Lead; Data curation: Equal; Formal analysis: Equal; Funding acquisition: Lead; Investigation: Equal; Methodology: Equal; Supervision: Equal; Writing – original draft: Lead; Writing – review & editing: Lead)

Conflicts of interest
The authors disclose no conflicts.

Funding
Aleixo M. Muise, Scott B. Snapper, Christoph Klein, Daniel Kotlarz, Eric Schadt, Carmen Argmann, and Dermot P.B. McGovern are funded by The Leona M. and Harry B. Helmsley Charitable Trust, and Aleixo M. Muise, Scott B. Snapper, Christoph Klein, Daniel Kotlarz, Eric Schadt, and Carmen Argmann are funded by the National Institutes of Health, National Institute of Diabetes and Digestive Kidney Diseases (NIDDK) (RC2DK122532). Aleixo M. Muise is funded by NIDDK (RC2DK118640), Canada Research Chair (Tier 1) in Pediatric IBD, and a Canadian Institutes of Health Research Foundation Grant. Jodie Ouahed and Dermot P.B. McGovern are supported by NIDDK (award numbers K08DK122133 and U01DK062413 respectively). DL, HY, and Zhiyang Zeng are funded by the National Natural Science Foundation of China (No.32025023) and by the Shanghai Municipal Commission for Science and Technology (No. 24J22800400). Daniel Kotlarz is also funded by the Deutsche Forschungsgemeinschaft (DFG, German Research Foundation; Heisenberg grant, KO 4891/6-1, 496078873; KO 4891/5-1, 447562338), Helmholtz Initiative and Networking Fund of the Helmholtz Association (Helmholtz Young Investigator Group, VH NG 1716), Else Kröner Fresenius Stiftung (Key Project 2019_A136), the Federal Ministry of Research, Technology and Space (Bundesministerium für Forschung, Technologie und Raumfahrt; BMFTR) as part of the German Center for Child and Adolescent Health (DZKJ) (funding code 01GL2406A; also to Christoph Klein), and Care for Rare Foundation. Xiang Shen is funded by China Scholarship Council (201909110092), Klinikum LMU, and Care-for-Rare Foundation. Ziqi Yu is also funded by China Scholarship Council (202008360174) Klinikum LMU, and Care-for-Rare Foundation. Tom Le Voyer is supported by the MD-PhD program of the Imagine Institute (with support from the Fondation Bettencourt-Schueller), and a "Poste CCA-INSERM-Bettencourt" (with support from the Fondation Bettencourt-Schueller). Funding was also provided by the Lassonde Family Precision IBD Initiative.

Data Availability
The identified *BIRC3* variants have been submitted to the ClinVar database (https://www.ncbi.nlm.nih.gov/clinvar/) with the IDs SCV006100892—SCV006100899. Human sequencing is not made publicly available because it contains information that could compromise research participant privacy/consent; however, it will be available to researchers upon request. Zebrafish and mice RNA sequencing data are available at public repository— Gene Expression Omnibus accession GSE299375.